energies

MDPI

Article

Investigation of Thermal-Flow Characteristics of Pipes with Helical Micro-Fins of Variable Height

Piotr Bogusław Jasiński, Michał Jan Kowalczyk, Artur Romaniak, Bartosz Warwas *, Damian Obidowski and Artur Gutkowski

Institute of Turbomachinery, Lodz University of Technology, 90-924 Lodz, Poland; piotr.jasinski@p.lodz.pl (P.B.J.); michal.kowalczyk.1@dokt.p.lodz.pl (M.J.K.); artur.romaniak@dokt.p.lodz.pl (A.R.); damian.obidowski@p.lodz.pl (D.O.); artur.gutkowski@p.lodz.pl (A.G.)

* Correspondence: bartosz.warwas@dokt.p.lodz.pl; Tel.: +48-42-631-23-71

Abstract: The results of numerical investigations of heat transfer and pressure drops in a channel with 30° helical micro-fins are presented. The main aim of the analysis is to examine the influence of the height of the micro-fins on the heat-flow characteristics of the channel. For the tested pipe with a diameter of 12 mm, the micro-fin height varies within the range of 0.05–0.40 mm (with 0.05 mm steps), which is equal to 0.4–3.3% of its diameter. The analysis was performed for a turbulent flow, within the range of Reynolds numbers 10,000–100,000. The working fluid is water with an average temperature of 298 K. For each tested geometry, the characteristics of the friction factor $f(Re)$ and the Nusselt number $Nu(Re)$ are shown in the graphs. The highest values of Nusselt numbers and friction factors were obtained for pipes with the micro-fins H = 0.30 mm and H = 0.35 mm. A large discrepancy is observed in the friction factors $f(Re)$ calculated from the theoretical relationships (for the irregular relative roughness values shown in the Moody diagram) and those obtained from the simulations (for pipes with regular roughness formed by micro-fins). The *PEC* (Performance Evaluation Criteria) heat transfer efficiency analysis of the geometries under study is also presented, taking into account the criterion of the same pumping power. The highest *PEC* values, reaching 1.25, are obtained for micro-fins with a height of 0.30 mm and 0.35 mm and with Reynolds numbers above 40,000. In general, for all tested geometries and for large Reynolds numbers (above 20,000), the *PEC* coefficient reaches values greater than 1, while for lower Reynolds numbers (less than 20,000), its values are less than 1.

Keywords: heat transfer coefficient; micro-fins; friction factor; numerical methods; CFD

Citation: Jasiński, P.B.; Kowalczyk, M.J.; Romaniak, A.; Warwas, B.; Obidowski, D.; Gutkowski, A. Investigation of Thermal-Flow Characteristics of Pipes with Helical Micro-Fins of Variable Height. *Energies* **2021**, *14*, 2048. https://doi.org/10.3390/en14082048

Academic Editor: Pouyan Talebizadeh Sardari

Received: 12 March 2021
Accepted: 2 April 2021
Published: 7 April 2021

1. Introduction

The pipe, as a flow channel, is one of the simplest and most commonly used in power engineering and thermal devices. It is widely applied in heat exchangers and to transport the medium in installations. The phenomena occurring in it are related to both fluid mechanics and thermal processes; therefore, the key issue is to design the geometry in such a way as to maximize heat transfer while limiting a negative effect of flow resistance.

There are many methods to intensify the heat transfer process in the pipe. Among others, intensifying inserts of various shapes and other flow turbulence devices are widely used. Wijayanta et al. [1] conducted a numerical study to evaluate the thermal hydraulic performance of a turbulent flow inside a tube equipped with a square-cut twisted tape and a classical twisted tape insert. In the range of Reynolds number from 8000 to 18,000 under investigation, the tube with a square-cut twisted tape had the highest values of heat transfer rate, friction factor, and thermal performance factor for the twisted ratio y/W = 2.7. In [2], Wijayanta et al. investigated the thermal performance of a tube heat exchanger with punched delta-winglet vortex generators. The numerical studies for Re = 9100–17,400 and the attack angles of 30°, 50°, and 70° allowed one to determine values of the Nusselt number, friction factor, and thermal performance factor, which increased with an increasing value

of attack angle. Jasiński [3–5] conducted experimental and numerical investigations of a flow in the circular tube with ball turbulators. The investigations for different diameters of the balls, different distances between them, and *Re* = 10,000–300,000 were carried out. The results showed that the highest increase in the Nusselt number and the friction factor was observed for the insert ball with largest diameters; however, the highest values of thermal performance factor were observed for the smallest balls. Arjmandi et al. [6] conducted a numerical investigation of applying twisted tape turbulator and Al_2O_3/water nanofluid in double pipe heat exchanger. The studies of heat transfer coefficient and pressure drop were carried out for different pitches ratios 0.09–0.18, angles 0–30°, and Reynolds numbers in the range 5000–20,000. According to obtained results, the optimization accomplished by the response surface methodology was performed, thanks to which the optimal vortex generator geometry was created.

Another method to intensify heat transfer is to apply nano-liquids as a modification of the working fluid. Patil et al. [7] made a review and presented investigations on synthesis, thermo-physical properties, and a heat transfer mechanism of nanofluids. Shajahan et al. [8] carried out experimental studies with a combination of nanofluids and inserts under the conditions of laminar flow. The results allowed for the determination of highest values of the Nusselt number, friction factor, and thermal performance factor according to different twist ratios of inserts and various types of nanofluids. Kristiawan et al. [9] investigated numerically an influence of micro-fins and TiO_2/water nanofluids on thermo-hydraulic performance. The highest *PEC* (Performance Evaluation Criteria) achieved the squared mini-channel with micro-fins and the nanoparticle concentration of 0.01 vol.%. Asirvatham et al. [10] presented the results of experimental studies of convective heat transfer with a low volume fraction of the CuO/water nanofluid. According to the gained experimental data, a correlation for the Nusselt number was evolved.

The third method of heat transfer intensification is surface finning, which is considered in this article. The problem of similar geometry has been already addressed widely in the scientific literature. In most cases, researchers perform experimental investigations, but an increasing number of publications based on combined numerical and experimental tests is observed. For example, Mann and Eckels [11], in order to improve heat transfer and reduce a pressure drop, optimized the following geometrical pipe parameters: the number of fins, their height and helical angle, for a Reynolds number ranging from 30,000 to 60,000. They used the ANSYS Fluent software and the NSGA II algorithm in the study. After comparing the numerical results with the experimental results, the researchers concluded that for helical angles above 45°, the relationship between heat transfer and geometry was chaotic rather than ordered. Wen-Tao et al. [12] conducted an experiment for a developed turbulent flow in the Reynolds number range from 10,000 to 100,000, for 16 different pipes with internal grooves. They compared the experimental results with the analytical method using the Gnielinski equation, which was then extended by the Nusselt number. The proposed extended equation yielded a good agreement of the results, where the deviation for 93% of the data was within ±20%.

Li et al. [13] used PIV (Particle Image Velocimetry) technology in the experimental investigations. They determined a relationship between flow characteristics and heat transfer for the geometry of a micro-finned rectangular duct. They observed an influence of the formation of coherent structures in the fluid on an increase in the heat transfer coefficient. Additionally, for low Reynolds numbers, characteristic of the laminar and transitional flow, they observed a lack of vortices filling the spaces between the fins, which was equivalent to the deterioration of heat transfer. Guo-Dong et al. [14] compared the experimental results for a plain pipe with an internally finned pipe using the (HMiM) BF_4 medium (1-hexyl-3-methyl-imidazolium-tetrafluoroborate). Based on the obtained results, they determined empirical coefficients to calculate a friction coefficient and a heat transfer coefficient for a laminar flow (*Re* = 60–600). Brognaux et al. [15] developed the characteristics of a single-phase flow through the pipe with two types of internal fins. They analyzed an influence of geometry on the Prandtl number and determined a dependence

of the Reynolds number on the friction coefficient. On the basis of experimental results, they observed that the Prandtl number exponent agreed well with other correlations for the geometry with two-dimensional roughness.

Jasiński [16] used numerical simulations to model a flow in the internally finned pipe for various helical angles of the micro-fins in the range of 0–90°. Using the EGM (Entropy Generation Minimization) method to assess the flow, he showed that for each geometry, the minimum entropy was generated for the range Re = 60,000–90,000. Tang and Li [17] developed a correlation of the friction coefficient for data from various experiments. The data include old and new refrigerants that were used in internally finned tube heat exchangers. Jensen and Vlakancic [18] compared the experimental results for different geometries of internally fined pipes and compared them with theoretical relationships. They developed an empirical correlation to calculate the friction coefficient and the Nusselt number. The developed criteria differed for high fins and micro-fins, which allowed for the appropriate use of the resulting correlations depending on the geometry of the pipe. Dastmalchi et al. [19] optimized the geometry of micro-finned tubes using numerical methods to increase heat transfer and minimize flow resistance. The research concerned double pipe heat exchangers during the turbulent flow. In the study, they changed the geometric parameters of the pipe, i.e., its internal diameter, number of fins, fin height and their helix angle, for various Reynolds numbers from 3000 to 100,000. Among other findings, the authors noted that the optimal micro-fin height increases with an increasing Reynolds number for all internal pipe diameters considered. In addition, Dastmalchi et al. [20] conducted oil flow tests with low Reynolds numbers, ranging from 100 to 1000, in a tube with internal micro-fins. As before, they investigated an influence of the tube geometry on heat transfer efficiency and pressure drop during flow. The sample results for Re = 1000 show the maximal heat transfer increase of 44%, but also a 69% increase in the friction coefficient, for the flow through micro-finned tubes compared to smooth tube flow.

Filho and Jabardo [21] investigated an influence of the geometry of three selected types of pipes: smooth, micro-finned, and herringbone on the thermo-hydraulic flow characteristics with the use of refrigerants. On the basis of the conducted research, they found that the thermal efficiency was the best for the herringbone pipe; however, it had the highest pressure drop. Raj et al. [22] investigated the properties of various types of internally and externally finned pipes for two fluids: water and 46% glycol solution. They showed that the Prandtl number had a large impact on the intensification of heat transfer, and at the same time, it was dependent on the temperature of fluids.

The present paper attempts to investigate the problem of thermal efficiency of several pipe geometries with micro-fins. By changing the height of inner fins, the researchers searched for the highest values of the *PEC* coefficient while maintaining the same pumping power. The tests were performed using numerical simulations, whereas for one pipe geometry, experimental tests were carried out as well. The paper presents in detail and discusses an influence of the height of micro-fins on the friction factor, heat transfer, and thermal efficiency of pipes, as well as a correlation of these parameters with mathematical functions. The main goal of this article, which provides the novelty, was the discovery of the best geometry of a pipe in terms of thermal efficiency by determining the highest value of PEC coefficient.

2. Materials and Methods

2.1. Experimental Stand

Before the numerical simulations were carried out, one of the pipe geometries was tested on the experimental stand by Zawadzki et al. [23], and the results obtained from the experiment were used to validate the numerical model. The object of the investigations was an internal finned pipe, produced industrially by KME Germany AG & Co. KG under the working name "TECTUBE fin 12736CV50/65D" and with the dimensions shown in Figure 1, which is used for the production of both single-phase and two-phase heat exchangers, e.g., evaporators in the refrigeration equipment.

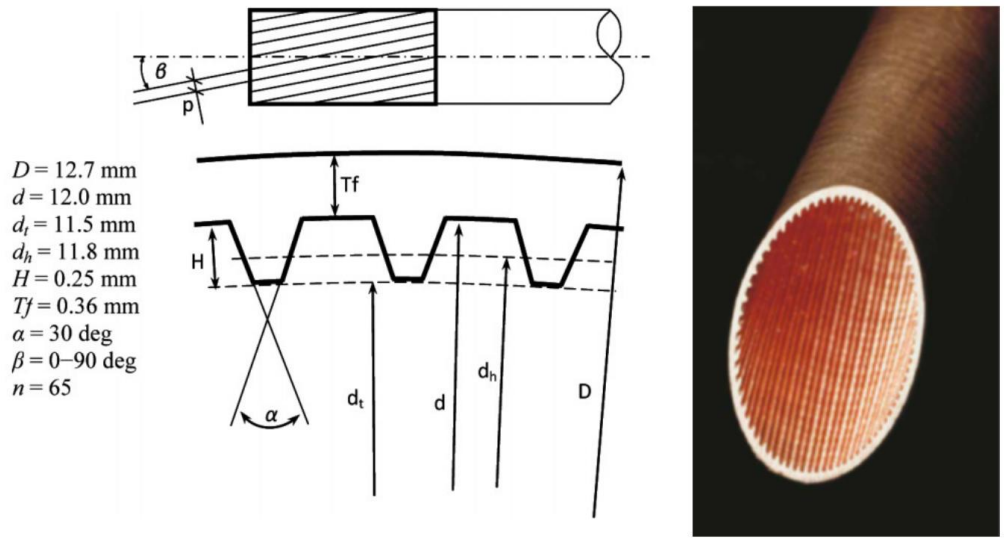

Figure 1. Scheme and dimensions of the micro-finned tube "TECTUBE fin 12736CV50/65D" produced by KME Germany AG & Co. KG company.

A schematic diagram of the experimental stand on which the test was performed is presented in Figure 2. The list of used devices in the experimental stand is introduced in Table 1. It consists of cold and hot water circulations, a data acquisition system, and a test section, which is a double pipe heat exchanger. During the measurements, constant temperatures in the circulation of cold and hot water were maintained at the inlets to the exchanger. In order to obtain thermal-flow characteristics, the water flow rate was gradually changed within the range of Reynolds numbers 10,000–60,000.

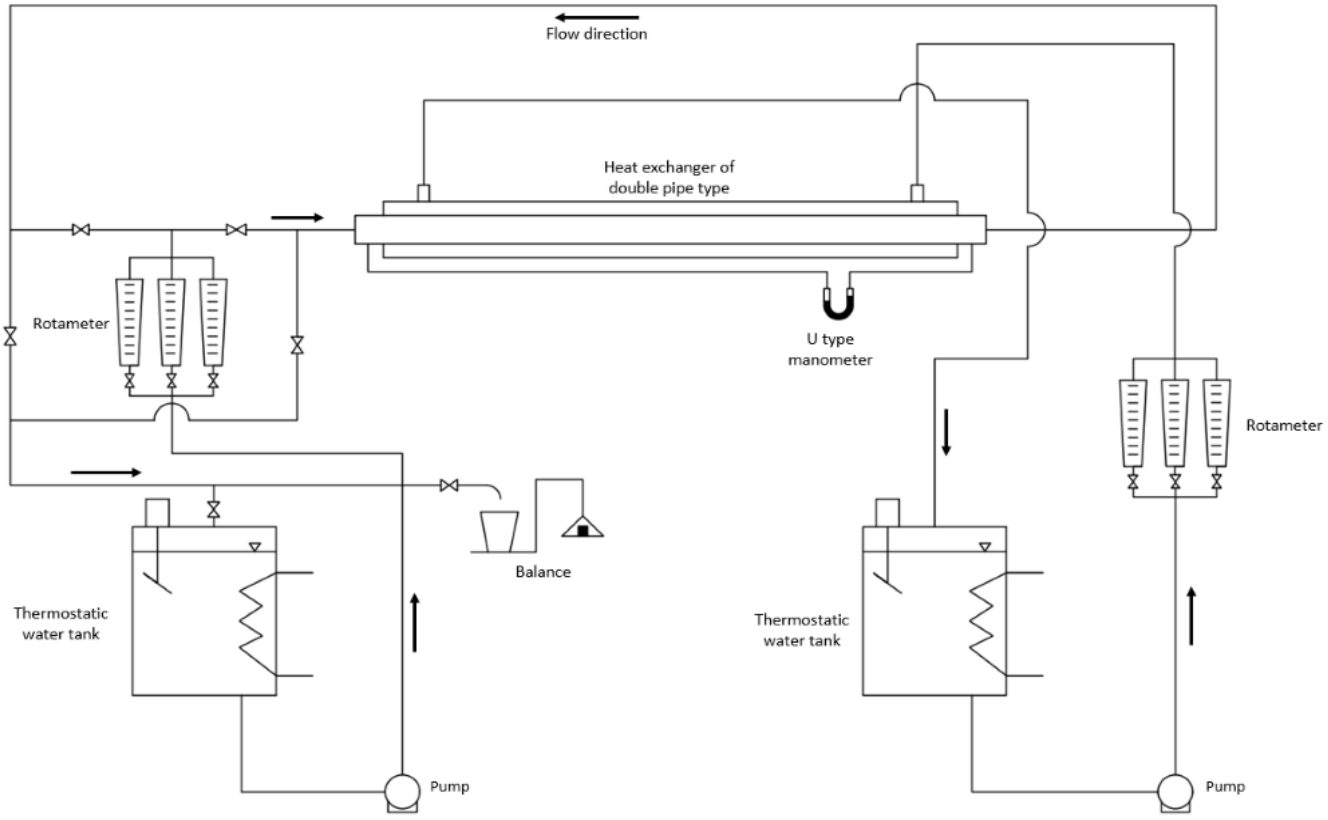

Figure 2. Experimental stand scheme for measuring micro-finned tubes [23].

Table 1. List of content used in experimental stand.

Legend Name	Type	Parameter	Operating Range
Balance	ZAO Gdansk—WT 1002	Weight [g]	10–1000 g
Thermostatic water tank	MLW—U10	Temperature [°C]	20–90 °C
Rotameter	Yokogawa—310142/002	Flow [l/h]	0–25 L/h
Pump	Lowara—2HMS4T/A	Flow rate [l/min]	20–70 L/min
U type manometer	Metalchem—MUR 1200	Pressure [Pa]	782.62–11,739.25 Pa

In Figure 3, the results of the experiment and numerical tests for the micro-finned tube from the previous studies are shown. This procedure also verified the two most popular turbulence models—the classic k-ε and the SST k-ω (Shear Stress Transport). It can be clearly seen that the best fit data and a good agreement with the experimental values for both pressure drop and heat transfer were obtained with the SST k-ω turbulence model. This is the reason why that model was used for further numerical calculations presented in this paper.

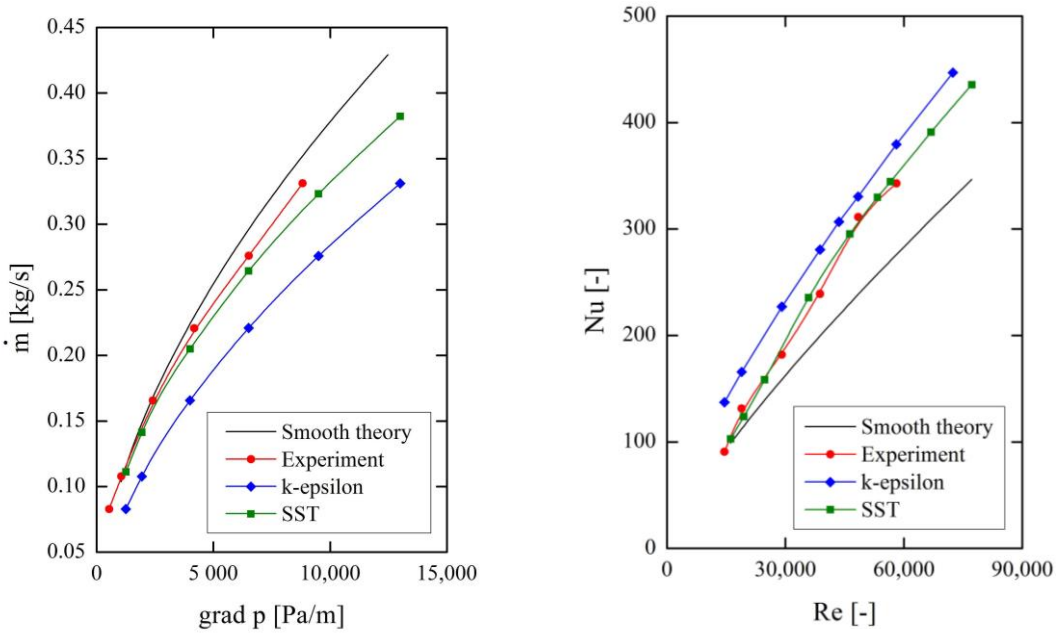

(**a**) (**b**)

Figure 3. Comparison between results of the simulation and the experiment for the micro-fin tube and the SST and k-ε turbulence model: (**a**) mass flow vs. *grad p*, (**b**) *Nu* vs. *Re* [16,24].

2.2. Geometrical Model

The aim of the numerical calculations was to investigate the thermal-flow characteristics of pipes with internal micro-fins, with a very similar geometry as shown in Figure 1 for the industrial pipe "TECTUBE fin 12736CV50/65D". The only geometric parameter that was changed was the height of the micro-fin H. All other parameters, including the fin helix angle $\alpha = 30°$ and the helical tooth line angle $\beta = 30°$, remained unchanged, as in the mentioned real pipe. Modifications of the tooth height H were made every 0.05 mm in the range of 0.05–0.40 mm, changing its size in relation to the height $H = 0.25$ mm, which the actual pipe has (see Figure 4). The relative roughness of the pipe, which is defined as the ratio of the height of unevenness on the surface of the pipe to its diameter $\varepsilon = H/d$ changes with a change of the micro-fin height. In this case, the "unevenness" are micro-fins of a given height H. Table 2 lists all the fin heights tested, together with the corresponding relative roughness ε. The models of selected cases are shown in Figure 5.

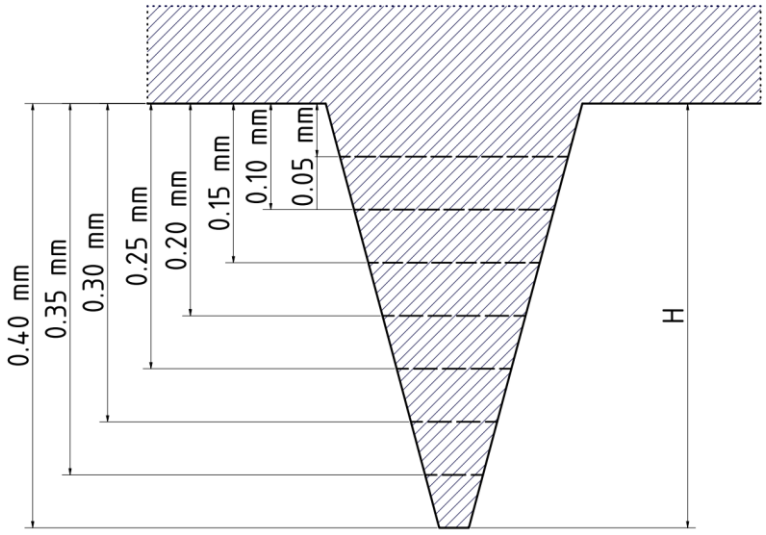

Figure 4. Scheme of changes in the fin height tested in the simulation.

Table 2. Results of the calculations of relative roughness.

***H* [mm]**	**0.05**	**0.10**	**0.15**	**0.20**	**0.25**	**0.30**	**0.35**	**0.40**
ε [-]	0.004	0.008	0.013	0.017	0.021	0.025	0.029	0.033

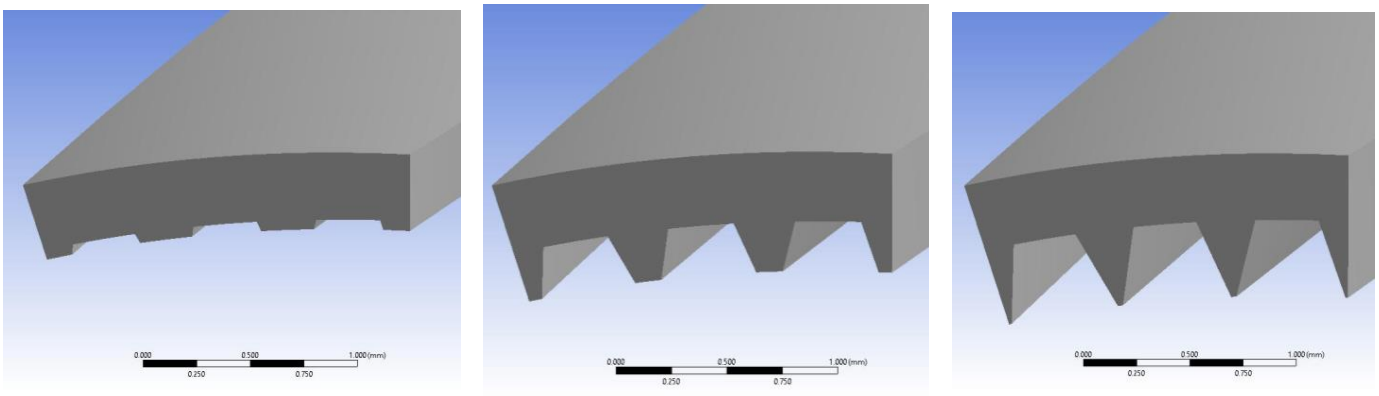

(**a**) (**b**) (**c**)

Figure 5. Different height of fins in the tube fragment model. (**a**) H = 0.05 mm, (**b**) H = 0.25 mm, (**c**) H = 0.40 mm.

2.3. Numerical Model

As the computational domain, a part of the spiral extruded pipe geometry was used, with a width of three fins as in Figure 5 and a length corresponding to its single helix pitch through an angle of 360° (Figure 6). The use of the width of three fins was due to the more convenient procedure of generating a computational mesh, which allowed us to maintain its better geometrical quality (cells angles, aspect ratio, etc.) in the central part of the channel near its axis, than for the width of one fin, but also applicable in such geometry. The list of used boundary conditions is introduced in Table 3.

Generally, instead of a full, long pipe, a repeating and periodic fragment of it, representative of the entire channel and reflecting the same heat-flow phenomena, was used for the calculations. This approach to the problem is correct, and it is commonly used in the numerical analysis [25,26], as long as the resulting flow is fully developed, both hydraulically and thermally. It is known that under normal conditions, a fully developed flow can be obtained only on a pipe length equal to approximately 40–50 diameters from its inlet. In the

case of using a short repeating domain fragment, appropriate boundary conditions have to be applied to obtain such a flow structure. According to this, translational periodicity was used at the inlet and outlet of the domain, where the fluid flow was forced by a pressure gradient, corresponding to the range of numbers Re = 10,000–100,000. Due to the twist of the micro-fins by an angle of 30°, there is also a component of the rotational velocity during the flow. Therefore, the rotational periodicity was used on the flank surfaces instead of the normal plane of symmetry. The concept of reducing the domain size, and thus also the number of computational mesh nodes, enables a significant reduction in computation time while maintaining high mesh quality and accuracy of results. This method of investigations has also been presented in [24,27,28].

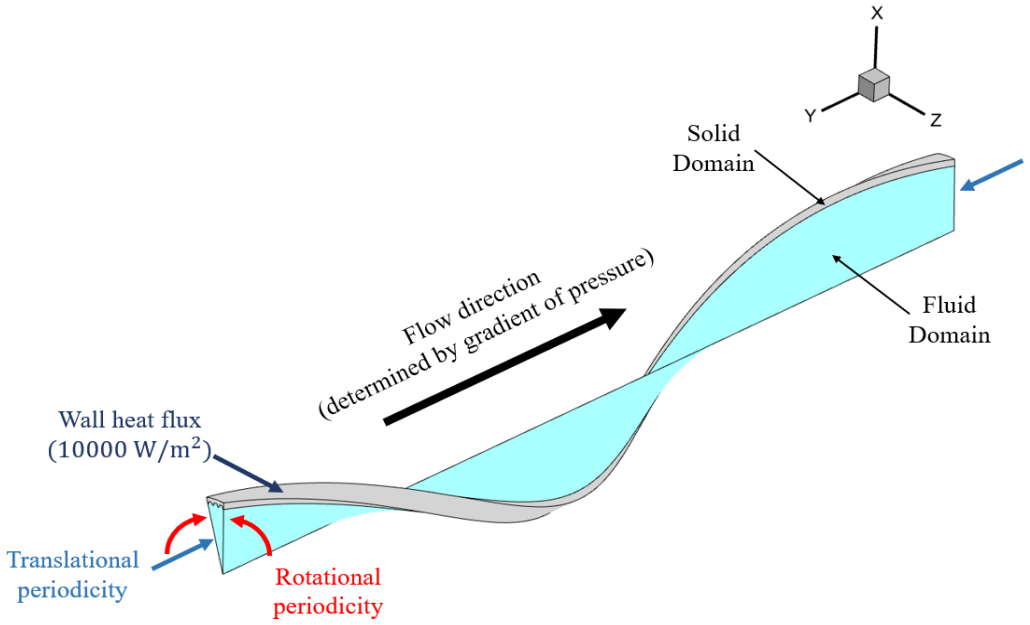

Figure 6. Boundary conditions on the models.

Table 3. Boundary conditions and the parameters values.

Boundary Condition	Description	Parameter	Value/Type
Fluid Domain	Water	Temperature Reference pressure Turbulence	298 K 1 atm SST
Subdomain	Subdomain was set in domain of water. The gradient of pressure determined the flow in Y component.	Gradient of pressure Volumetric heat flux	440–24,779 Pa $-Q_{vol} = \frac{q \cdot A_{wall}}{V_{water}}$ W
Solid Domain	Copper	Temperature	298 K
Wall	Boundary condition set on exterior area of pipe in the form of constant heat flux	Heat flux	10,000 $\frac{W}{m^2}$
Translational periodicity	Translational periodicity set on the inlet and outlet areas of fluid and solid domain.	-	-
Rotational periodicity	Rotational periodicity set on the both sides of fluid and solid domain. As the rotation axis, Global Y was set.	-	-

The pipe segment forming the computational domain was "extended" to the length of a full revolution, as shown along with other boundary conditions in Figure 6. As previously mentioned, the boundary condition forcing the fluid flow was a pressure gradient.

The simulation was conducted in Ansys CFX 2020 R2. The numerical model consisted of two computational domains. In the flow domain, water is defined as the working fluid with an average temperature of 298 K. The solid-state domain was defined as copper, which is the pipe material in the experiment. Additionally, a negative volumetric heat source

was set in the fluid domain to obtain a fully thermally developed flow and to calculate the correct temperature field. This solution made it possible to balance the thermal energy supplied to the domain wall as a heat flux of q = 10,000 W/m^2.

The SST k-ω turbulence model is one of the most popular models used in many CFD (Computational Fluid Dynamics) applications. Its main attribute is the ability to solve the viscous sublayer by applying the k-ω model near the wall and the standard k-ε model in the turbulent core area. Switching between the two models is controlled by a special built-in blending function [29,30]. Correct use of the SST model requires several mesh nodes inside the turbulent sublayer to maintain the condition of dimensionless distance $y^+ < 2$ in the entire boundary layer of the computational domain [31]. In the results presented in this work, the maximum value of y^+ did not exceed the mentioned value in any of the geometries.

One of the criteria for the uniqueness of the numerical solution was to achieve the appropriate convergence for residues: momentum, energy, and turbulence. In all simulations, a convergence of 1×10^{-4} or maximal residuals and an order of magnitude lower (1×10^{-5}) for mean RMS (Root-Mean-Square) residuals were obtained. The second criterion for the uniqueness of the solution was the stabilization of flow-thermal parameters, such as velocity, pressure, and temperature, which were monitored both as mean values and in several selected points in the computational domain. The computation process was finished if the above parameters did not change for several consecutive iterations.

Before the actual simulations, checking calculations were performed for different mesh qualities. For further calculations, a structural (in solid) and hexagonal mesh of such density, at which its further densification gives results differing less than 1%, was selected. For all geometries, efforts were made to maintain a computational mesh of approximately the same average cell volume. In the area of the hydraulic boundary layer, the mesh was additionally compacted to obtain the appropriate y^+ value. After the test, it can be concluded that the mesh used and the test results are independent of its density, which is consistent with the recommendations in [32]. The obtained value of the GCI (Grid Convergence Method) parameters in relation to the average temperature is GCI_{fine} = 1.8%, and in case of the wall heat flux, it is GCI_{fine} = 0.001%.

In Figure 7, the mesh used for the numerical calculations for H = 0.25 mm is shown.

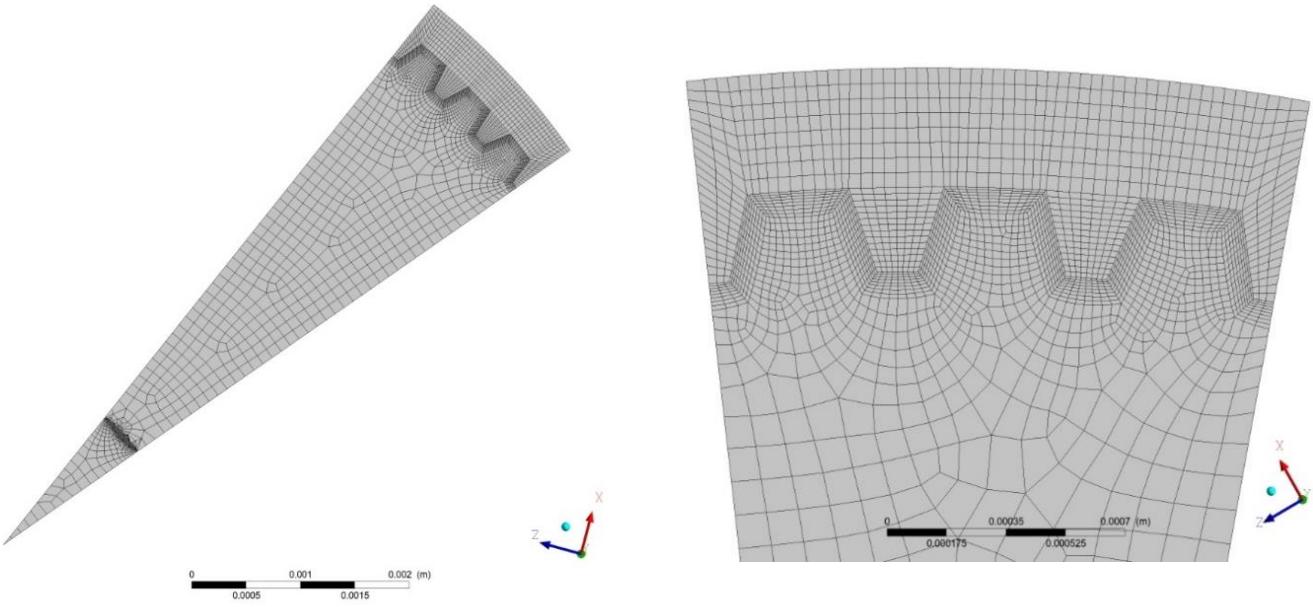

(**a**) (**b**)

Figure 7. Mesh used in the numerical simulations for H = 0.25 mm: (**a**) full view of mesh; (**b**) mesh region between solid and fluid domain.

3. Results

After performing numerical simulations, the correctness of the obtained results was assessed by analyzing the distribution of selected physical quantities. In Figure 8, results from the numerical simulations are shown. The contours of temperature and vectors of velocity distributions are presented for the cases in Figure 5, respectively.

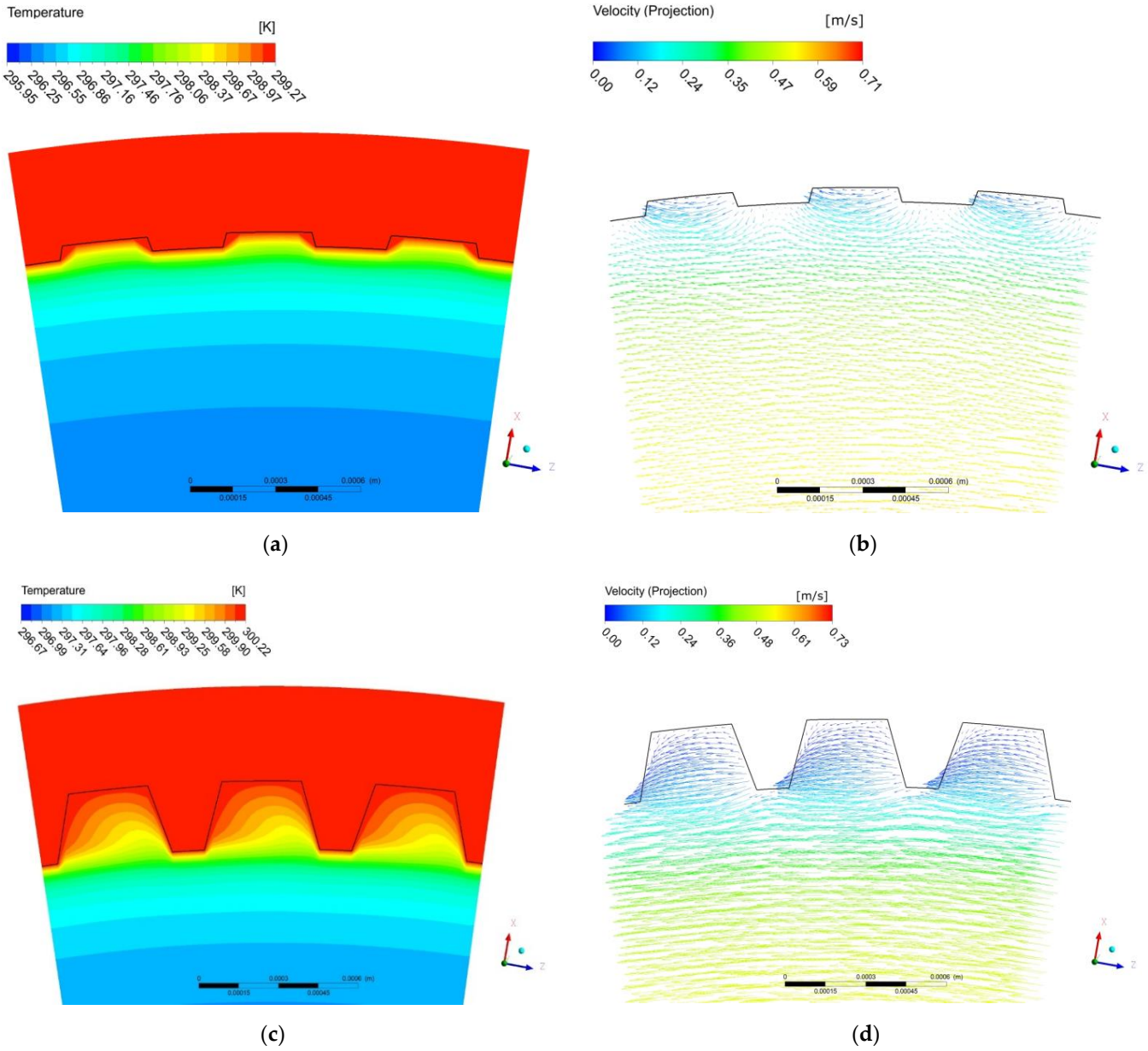

Figure 8. *Cont.*

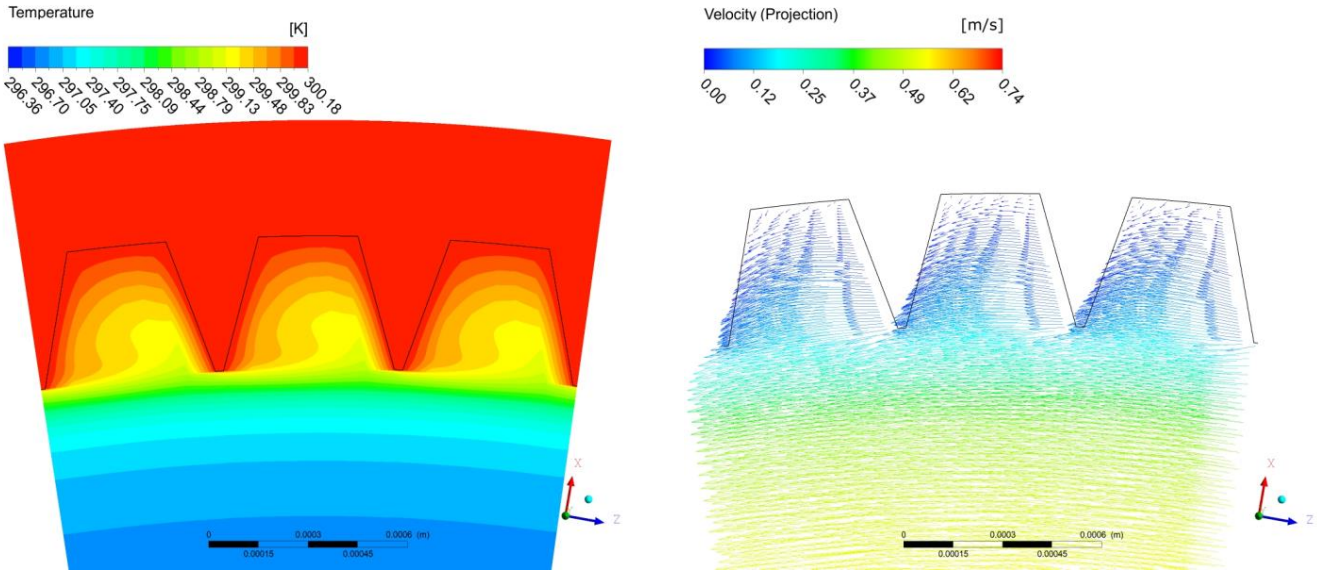

(**e**) (**f**)

Figure 8. Results from the numerical simulations: (**a**) contour of temperature for H = 0.05 mm; (**b**) vectors of velocity (tangential projection) for H = 0.05 mm; (**c**) contour of temperature for H = 0.25 mm; (**d**) vectors of velocity (tangential projection) for H = 0.25 mm; (**e**) contour of temperature for H = 0.40 mm; (**f**) vectors of velocity (tangential projection) for H = 0.40 mm.

3.1. Data Processing

Based on the experimental data obtained from the examination of the industrial pipe TECTUBE fin 12736CV50/65D, the numerical model was validated and verified. The most important parameters in terms of the performance of the analyzed pipes are the friction factor and the heat transfer coefficient, as expressed by the Nusselt number. To create such characteristics, it is necessary to define basic flow parameters such as velocity, temperature, and pressure drop for each pipe geometry, which were obtained as a result of the computer simulations.

In numerical calculations, the pressure gradient described by Equation (1) was used to force the flow:

$$grad\ p = \frac{\Delta p}{L} = f \cdot \frac{u_{av}^2 \cdot \rho}{2 \cdot d}. \quad (1)$$

For each tested geometry, the friction factor was calculated using the Darcy–Weisbach Equation (2), which is a modification of Equation (1):

$$f = \frac{2 \cdot \Delta p \cdot d}{\rho \cdot u_{av}^2 \cdot L}. \quad (2)$$

The theoretical value of the friction factor for a plain pipe, as the reference level for the numerical results, was calculated from the Blasius correlation (3):

$$f_{plain} = 0.3164 \cdot Re^{-0.25}. \quad (3)$$

Similarly, for the plain pipe, the Nusselt number was calculated from the well-known Dittus–Boelter [33,34] Equation (4):

$$Nu_{plain} = 0.023 \cdot Re^{0.8} \cdot Pr^{0.4}. \quad (4)$$

For the investigated cases of a finned tube, the formula (5) was used to calculate the Nusselt number:

$$Nu = \frac{h \cdot d}{k}. \tag{5}$$

The heat transfer coefficient h used in Equation (5) was determined from the formula for heat flux (6), from the obtained results of the numerical tests.

$$h = \frac{q}{T_{wall} - T_{bulk}} \tag{6}$$

3.2. Friction Factor

The results of numerical simulations, in the form of the characteristics of the friction factor $f(Re)$, are shown in Figure 9. The graph also features a curve for a smooth pipe, which was calculated from the Blassius correlation (3), to show the reference level.

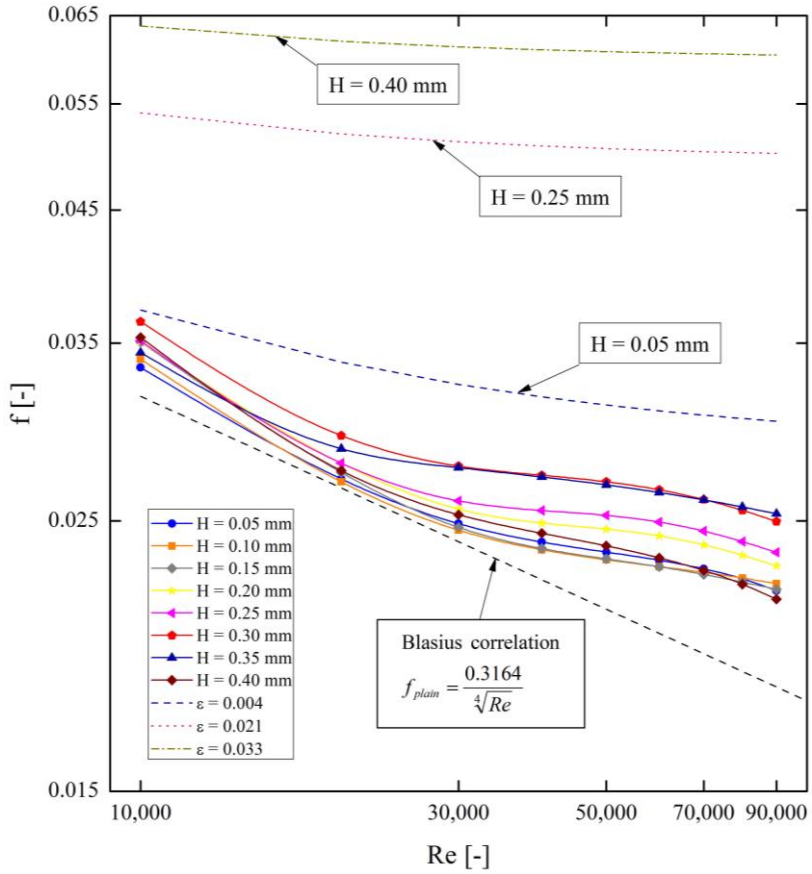

Figure 9. Results from the numerical simulations for various fin heights in the tube—f vs. Re.

It is difficult to find any simple approximation function that would express the variation in the height of micro-fins with a mathematical formula. For this reason, the friction factor was approximated separately for each pipe geometry, using an exponential third-order decay function (7), which makes the best fitting of the research results. The calculated correlation coefficients of the function are given in Table 4.

$$f = y_0 + A_1 \cdot \exp\left(\frac{Re}{t_1}\right) + A_2 \cdot \exp\left(\frac{Re}{t_2}\right) + A_3 \cdot \exp\left(\frac{Re}{t_3}\right) \tag{7}$$

Table 4. Fitting parameters for Equation (7). For all geometries coefficient, y_0 = 0.0208.

	***H* = 0.05**	***H* = 0.10**	***H* = 0.15**	***H* = 0.20**	***H* = 0.25**	***H* = 0.30**	***H* = 0.35**	***H* = 0.40**
A_1	0.02839	−0.2313	2.38×10^{-1}	−0.786	−0.2992	0.04275	0.6984	−0.5991
t_1	−8956	9.99×10^{6}	-1.50×10^{4}	-2.06×10^{4}	-3.03×10^{4}	-7.74×10^{3}	-9.73×10^{4}	3.24×10^{5}
A_2	0.1788	0.03154	−0.2564	0.5124	0.2837	0.3272	−0.6903	0.6042
t_2	1.34×10^{5}	-8.61×10^{3}	-1.76×10^{4}	-1.76×10^{4}	-3.27×10^{4}	-4.41×10^{4}	-9.68×10^{4}	3.33×10^{5}
A_3	−0.1754	0.2348	5.36×10^{-2}	0.3076	0.05362	−0.3259	0.05387	0.04127
t_3	1.30×10^{5}	-9.54×10^{92}	-2.78×10^{4}	-2.55×10^{4}	-1.04×10^{4}	-4.21×10^{4}	-4.53×10^{3}	-6.97×10^{3}

For the micro-fins of height H = 0.05 mm, H = 0.25 mm, and H = 0.40 mm (minimal, medium, and maximal micro-fin height, respectively) the curves were calculated for several ε values from Table 2, using the empirical formula (8) given by Swamee and Jain [35].

In Figure 10, an influence of the pipe geometry on a value of the friction factor $f(H)$ for several Reynolds numbers is shown. The individual curves show the friction factor with respect to micro-fins height H for specific Reynolds numbers, i.e., for the same flow parameters.

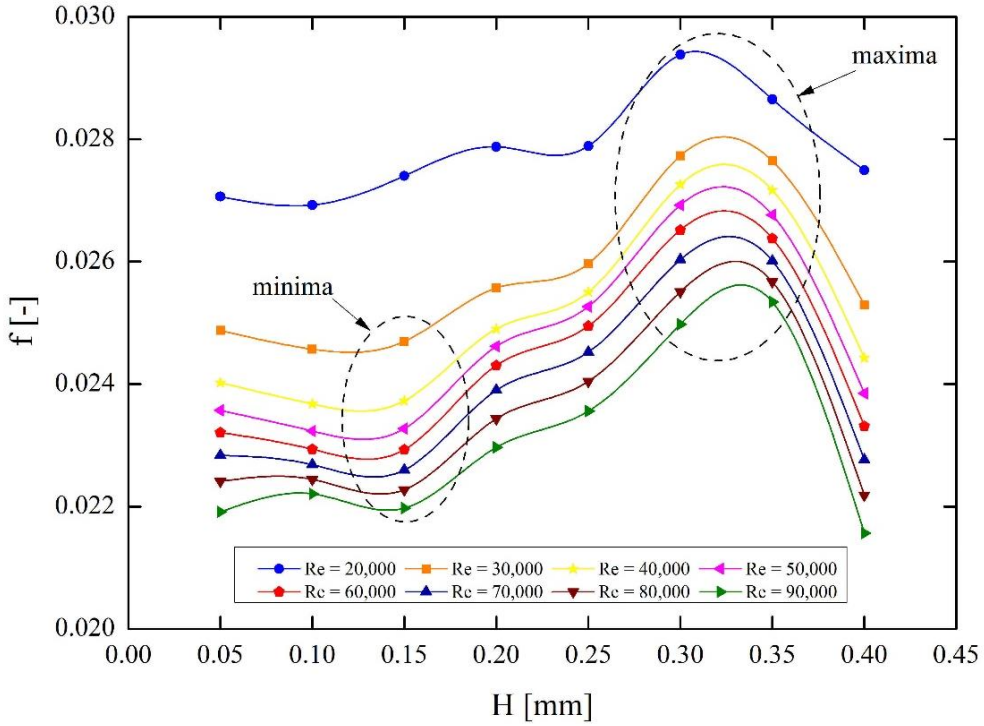

Figure 10. Results from the numerical simulations of the friction factor for various micro-fin heights in the tube—f vs. H (for a specific value of Reynolds Number).

An analysis of the obtained results allowed us to observe a large deviation from the characteristics of rough pipes presented in the Moody diagram [36]. In the case of pipes, the relative roughness is defined as a ratio of the height of unevenness to the diameter, and for the tested geometries, it is closely related to the height of the micro-fins. For the presented channels, it is 0.004–0.033, which was presented in Table 2.

$$f = \frac{0.25}{\left(\log\left(\frac{\varepsilon}{3.7} + \frac{5.74}{Re^{0.9}}\right)\right)^2} \quad (8)$$

3.3. Heat Transfer

In Figure 11, thermal characteristics for all tested geometries are shown, in the form of the *Nu*(*Re*) function, and one curve for a plain pipe, calculated from (4) as the reference level.

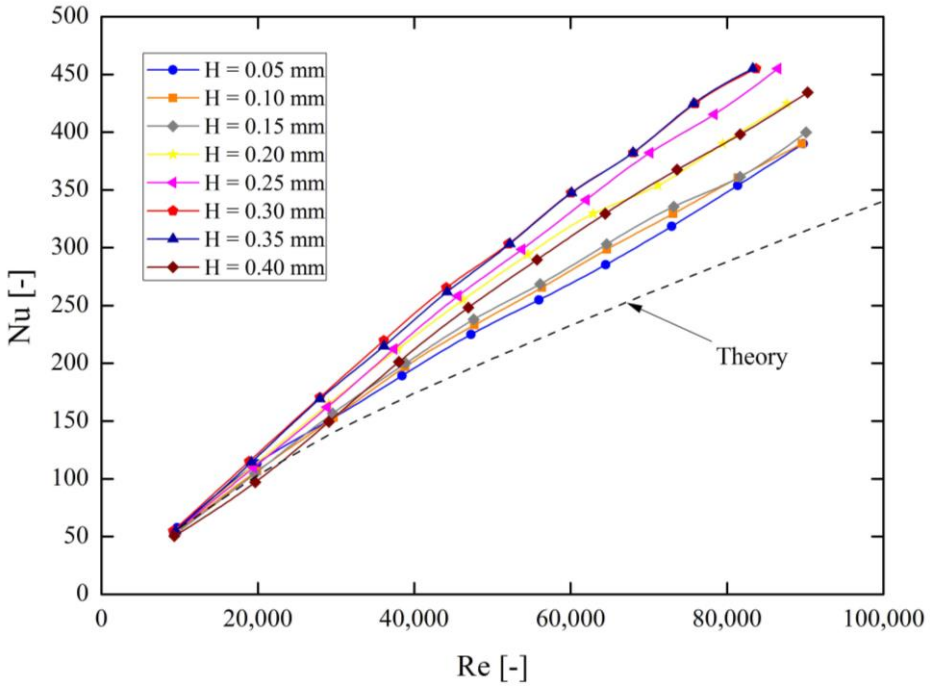

Figure 11. Results from the numerical simulations for various fin heights in the tube—*Nu* vs. *Re*.

Between the functions of Nusselt numbers shown in Figure 11, there is no simple geometric dependence (similar to the friction factor); nevertheless, certain mathematical functions can be adjusted to these data.

For the correlation of the Nusselt number function for the studied cases, the most suitable formula is the exponential function (9):

$$Nu = A \cdot Re^{B} \cdot Pr^{0.4}. \quad (9)$$

In Table 5, values of the *A* and *B* coefficients for each fin height are shown.

Table 5. Fitting parameters for Equation (9).

	***H* = 0.05**	***H* = 0.10**	***H* = 0.15**	***H* = 0.20**	***H* = 0.25**	***H* = 0.30**	***H* = 0.35**	***H* = 0.40**
A	0.014370	0.013610	0.013760	0.013940	0.006390	0.009170	0.007314	0.006306
B	0.8402	0.8470	0.8475	0.8544	0.9301	0.9014	0.9218	0.9242

3.4. PEC (Performance Evaluation Criteria)

The *PEC* (Performance Evaluation Criteria) thermal efficiency rating for the tested pipes was calculated from Equation (10). This parameter combines the Nusselt number and the friction factor obtained from the tests of channels with geometries other than the smooth pipe, and the *Nu* and *f* numbers calculated for a smooth pipe with the same Reynolds number. The *PEC* is an indicator of how the heat transfer will increase in the tested channel relative to a plain pipe for the same pumping power. *PEC* values above 1 indicate a greater impact of intensification of the heat transfer in the pipe than flow

resistance, while values below 1 indicate greater flow resistance in relation to the benefit obtained from intensifying the heat transfer for the tested geometry (Figure 12).

$$PEC = \frac{\frac{Nu}{Nu_{plain}}}{\left(\frac{f}{f_{plain}}\right)^{\frac{1}{3}}} \quad (10)$$

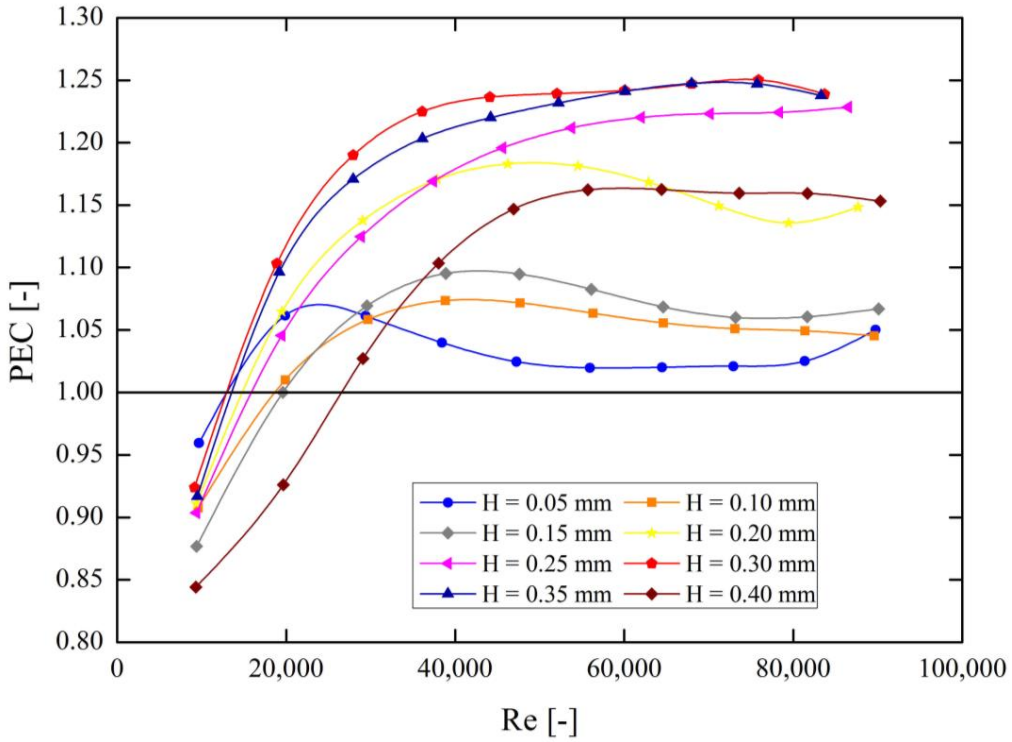

Figure 12. PEC (Performance Evaluation Criteria) coefficient of effectiveness for each tested model—*PEC* vs. *Re*.

4. Discussion

A validation of the numerical model with the experimental data from the tests for a pipe with the fin height of H = 0.25 mm was presented. When analyzing the results, the discrepancies between the experiment and the obtained numerical results found are as follows: for the friction factor—maximum 7%; for a Nusselt number—maximum 12%, as indicated in Figure 3.

Using the Blasius formula determining the friction factor, a comparison of the obtained numerical results for different micro-fin heights with the plain pipe was made (Figure 9). For each case of micro-finned pipes, the obtained values are greater than the values for a smooth pipe, which indicates the physical correctness of the results obtained. For Re = 10,000–25,000, the lowest values of the friction factor are achieved by the pipe with micro-fins of the height of H = 0.05 mm; whereas the highest values for the height of micro-fins are H = 0.30 mm. All curves are rather regular and straight lines on a logarithmic plot. For Reynolds numbers above 25,000, the lowest values of the friction factor are achieved by tubes with micro-fins of the height of H = 0.10 mm and H = 0.15 mm; in turn, the highest values are achieved by two geometries for pipes with micro-fins of the height of H = 0.30 mm and H = 0.35 mm. In this range, functions change their character, and it is difficult to find a regularity in their position.

Considering the dependence of the friction factor in relation to the fin height for different Reynolds numbers, its value decreases with an increase in the Reynolds number for each flow channel. On the basis of Figure 10, apart from minor irregularities in the charac-

teristics, one can notice their quite clear trend. For the micro-fins height H = 0.30–0.35 mm, a clear maximum can be seen for all the characteristics, which means that these pipe geometries give the highest flow resistance. On the other hand, for the height of approximately H = 0.15 mm, one can observe a "slight" minimum of these curves and a decrease in the value for the highest height of micro-fins H = 0.40 mm. The decrease in the value of the friction factor for H = 0.40 mm is probably due to low thickness of the fin compared to other dimensions (Figure 5). At the same time, a small contact area with the main turbulent core, where the highest flow velocities occur, exerts also an influence on a decrease in the friction factor.

Each tested tube had a different relative roughness related to the height of the micro-fins. In Figure 9, a complete discrepancy between the positions of the curves obtained from the numerical simulations and those calculated theoretically on the basis of the well-known formula (8) was shown for the same relative roughness. One can notice that it is not possible to calculate the friction factors from Equation (8) for the tested geometries as the model derives significantly different values than the ones obtained in the tests. Therefore, one of the fundamental conclusions resulting from the numerical tests carried out is a lack of correlation of the friction factor between the theoretically calculated (for irregular roughness) and the one obtained from the tests (for the same roughness but with regular shapes). The same fact was recognized by Wang et al. in their research [37].

When analyzing the obtained results of the heat transfer intensity for the geometries under investigation, several phenomena can be observed. The presented results show an irregular order of the Nusselt number characteristics for various fluid flow rates (Figure 11). For Reynolds numbers above 20,000, pipes with micro-fins having the height of H = 0.20 mm and higher achieve significantly larger values of the Nusselt number than for the plain pipe, compared to the cases with micro-fins below H = 0.20 mm, for which the characteristics are very similar to those of the smooth pipe. In the entire range of Reynolds numbers, the highest values of Nusselt numbers are achieved by pipes with micro-fin heights equal to H = 0.30 mm and H = 0.35 mm, and the same pipes for which the highest friction factor was observed. The irregular position of these characteristics indicates a significant influence of turbulences in the vicinity of the laminar boundary layer and the size of the heat transfer surface related to the height of the micro-fins.

As can be seen in Figure 12, in the range of low Reynolds numbers up to approximately 25,000, the *PEC* value of less than 1 was observed for all geometries. It means that using these pipes in this flow range is less efficient than using the regular plain pipe. For Reynolds numbers higher than 25,000, all characteristics are higher than 1, and it is within this range that the use of such pipes is justified. The highest *PEC* values, up to 1.25, are achieved by tubes with the micro-fin height of 0.30 and 0.35 mm for Reynolds numbers above 50,000. A characteristic feature of these geometries is a virtually constant value of this coefficient in the given Reynolds number range. Therefore, these micro-fins heights can be considered the most optimal for thermal-flow applications among all numerically tested in this work.

5. Conclusions

Based on the numerical investigations presented, the most important conclusions of this work can be drawn as follows:

- A numerical model of the tested pipes was built and verified with the experimental data.
- The mathematical correlations describing the nature of changes in the friction factor and the Nusselt number as a function of the Reynolds number were determined for the examined micro-fins heights.
- Using the PEC (Performance Evaluation Criteria) method of assessing the thermal efficiency of flow channels, the highest values were observed for micro-fins with the height of H = 0.30 mm and H = 0.35 mm.

- The theoretical formulas for the friction factor for rough pipes (Moody's diagram) were not compatible with the obtained numerical results for the same relative roughness, but with a regular shape.
- For Reynolds numbers below 20,000, the use of the investigated type of pipe micro-finning is unjustified in terms of heat transfer efficiency.

Author Contributions: Conceptualization, P.B.J., M.J.K., A.R., B.W., and D.O.; methodology, D.O.; validation, M.J.K., A.R., and B.W.; investigation, M.J.K., A.R., and B.W.; writing—original draft preparation, M.J.K., A.R., and B.W.; writing—review and editing, P.B.J. and A.G.; supervision, P.B.J. and A.G.; All authors have read and agreed to the published version of the manuscript.

Funding: This research received no external funding.

Institutional Review Board Statement: Not applicable.

Informed Consent Statement: Not applicable.

Data Availability Statement: Not applicable.

Acknowledgments: This article has been completed while the second, third, and fourth authors were Doctoral Candidates in the Interdisciplinary Doctoral School at the Lodz University of Technology, Poland. We would like to thank Malgorzata Jozwik for her significant linguistic help during the preparation of the manuscript.

Conflicts of Interest: The authors declare no conflict of interest.

Nomenclature

A_{wall}	exterior area of the pipe [m^2]
d	diameter [mm]
f	friction factor [-]
f_{plain}	friction factor for plain tube [-]
GCI_{fine}	fine-grid convergence index [%]
h	heat transfer coefficient [W/m^2K]
H	height of fin [mm]
k	thermal conductivity [W/mK]
L	length of the pipe [m]
Nu	Nusselt number [-]
Nu_{plain}	Nusselt number for plain tube [-]
PEC	performance evaluation criteria [-]
Δp	pressure drop [Pa]
Pr	Prandtl number [-]
Q_{vol}	volumetric heat flux [W/m^3]
q	wall heat flux [W/m^2]
Re	Reynolds number [-]
T_{wall}	average temperature in pipe [K]
T_{bulk}	minimal temperature in water [K]
u_{av}	average velocity [m/s]
V_{water}	volume of water domain [m^3]
α	micro-fin angle [°]
β	helical angle of micro-fin [°]
ρ	density [kg/m^3]
ε	relative roughness [-]

References

1. Wijayanta, A.T.; Pranowo; Mirmanto; Kristiawan, B.; Aziz, M. Internal flow in an enhanced tube having square-cut twisted tape insert. *Energies* **2019**, *12*, 306. [CrossRef]
2. Wijayanta, A.T.; Aziz, M.; Kariya, K.; Miyara, A. Numerical study of heat transfer enhancement of internal flow using double-sided delta-winglet tape insert. *Energies* **2018**, *11*, 3170. [CrossRef]

3. Jasiński, P.B. Numerical study of the thermo-hydraulic characteristics in a circular tube with ball turbulators. Part 1: PIV experiments and a pressure drop. *Int. J. Heat Mass Transf.* **2014**, *74*, 48–59. [CrossRef]
4. Jasiński, P.B. Numerical study of the thermo-hydraulic characteristics in a circular tube with ball turbulators. Part 2: Heat transfer. *Int. J. Heat Mass Transf.* **2014**, *74*, 473–483. [CrossRef]
5. Jasiński, P.B. Numerical study of thermo-hydraulic characteristics in a circular tube with ball turbulators. Part 3: Thermal performance analysis. *Int. J. Heat Mass Transf.* **2017**, *107*, 1138–1147. [CrossRef]
6. Arjmandi, H.; Amiri, P.; Pour, M.S. Geometric optimization of a double pipe heat exchanger with combined vortex generator and twisted tape: A CFD and response surface methodology (RSM) study. *Therm. Sci. Eng. Prog.* **2020**, *18*. [CrossRef]
7. Patil, M.S.; Seo, J.-H.; Kang, S.-J.; Lee, M.-Y. Review on synthesis, thermo-physical property, and heat transfer mechanism of nanofluids. *Energies* **2016**, *9*, 840. [CrossRef]
8. Shajahan, M.I.; Michael, J.J.; Arulprakasajothi, M.; Suresh, S.; Nasr, E.A.; Hussein, H.M.A. Effect of Conical Strip Inserts and ZrO 2 / DI-Water Nanofluid on Heat Transfer Augmentation: An experimental study. *Energies* **2020**, *13*, 4554. [CrossRef]
9. Kristiawan, B.; Wijayanta, A.T.; Enoki, K.; Miyazaki, T.; Aziz, M. Heat transfer enhancement of TiO2/water nanofluids flowing inside a square minichannel with a microfin structure: A numerical investigation. *Energies* **2019**, *12*, 3041. [CrossRef]
10. Asirvatham, L.G.; Vishal, N.; Gangatharan, S.K.; Lal, D.M. Experimental Study on Forced Convective Heat Transfer with Low Volume Fraction of CuO/Water Nanofluid. *Energies* **2009**, *2*, 97–119. [CrossRef]
11. Mann, G.W.; Eckels, S. Multi-objective heat transfer optimization of 2D helical micro-fins using NSGA-II. *Int. J. Heat Mass Transf.* **2019**, *132*, 1250–1261. [CrossRef]
12. Ji, W.-T.; Zhang, D.-C.; He, Y.-L.; Tao, W.-Q. Prediction of fully developed turbulent heat transfer of internal helically ribbed tubes? An extension of Gnielinski equation. *Int. J. Heat Mass Transf.* **2012**, *55*, 1375–1384. [CrossRef]
13. Li, P.; Campbell, M.; Zhang, N.; Eckels, S.J. Relationship between turbulent structures and heat transfer in microfin enhanced surfaces using large eddy simulations and particle image velocimetry. *Int. J. Heat Mass Transf.* **2019**, *136*, 1282–1298. [CrossRef]
14. He, G.-D.; Fang, X.-M.; Xu, T.; Zhang, Z.-G.; Gao, X.-N. Forced convective heat transfer and flow characteristics of ionic liquid as a new heat transfer fluid inside smooth and microfin tubes. *Int. J. Heat Mass Transf.* **2015**, *91*, 170–177. [CrossRef]
15. Brognaux, L.; Webb, R.L.; Chamra, L.M.; Chung, B.Y. Single-phase heat transfer in micro-fin tubes. *Int. J. Heat Mass Transf.* **1997**, *40*, 4345–4357. [CrossRef]
16. Jasiński, P. Numerical optimization of flow-heat ducts with helical micro-fins, using entropy generation minimization (EGM) method. In *Recently Advances in Fluid Mechanics and Heat & Mass Transfer, Proceedings of the 9th IASME/WSEAS International Conference on Fluid Mechanics and Aerodynamic Engineering FMA'11, Proceedings of the 9th IASME/WSEAS International Conference on HTE'11, Florence, Italy, 23–25 August 2011*; WSEAS: Athens, Greece, 2011; pp. 47–54.
17. Tang, W.; Li, W. Frictional pressure drop during flow boiling in micro-fin tubes: A new general correlation. *Int. J. Heat Mass Transf.* **2020**, *159*, 120049. [CrossRef]
18. Jensen, M.K.; Vlakancic, A. Technical Note Experimental investigation of turbulent heat transfer and fluid flow in internally finned tubes. *Int. J. Heat Mass Transf.* **1999**, *42*, 1343–1351. [CrossRef]
19. Dastmalchi, M.; Sheikhzadeh, G.A.; Arefmanesh, A. Optimization of micro-finned tubes in double pipe heat exchangers using particle swarm algorithm. *Appl. Therm. Eng.* **2017**, *119*, 1–9. [CrossRef]
20. Dastmalchi, M.; Arefmanesh, A.; Sheikhzadeh, G. Numerical investigation of heat transfer and pressure drop of heat transfer oil in smooth and micro-finned tubes. *Int. J. Therm. Sci.* **2017**, *121*, 294–304. [CrossRef]
21. Filho, E.P.B.; Jabardo, J.M.S. Experimental study of the thermal hydraulic performance of sub-cooled refrigerants flowing in smooth, micro-fin and herringbone tubes. *Appl. Therm. Eng.* **2014**, *62*, 461–469. [CrossRef]
22. Raj, R.; Lakshman, N.S.; Mukkamala, Y. Single phase flow heat transfer and pressure drop measurements in doubly enhanced tubes. *Int. J. Therm. Sci.* **2015**, *88*, 215–227. [CrossRef]
23. Zawadzki, A.; Plocek, M.; Kapusta, T.; Kasieczka, W. Heat transfer and friction factor characteristics of single-phase flow through a circular, internally micro-finned, horizontal tube fitted with twisted tape inserts—experimental investigations. In Proceedings of the XL Refrigeration Days, Poznań, Poland, 15–17 October 2008; pp. 115–124. (In Polish)
24. Jasiński, P. Numerical Study of Friction Factor and Heat Transfer Characteristics for Single-Phase Turbulent Flow in Tubes with Helical Micro-Fins. *Arch. Mech. Eng.* **2012**, *59*, 469–485. [CrossRef]
25. Sobczak, K.; Obidowski, D.; Reorowicz, P.; Marchewka, E. Numerical investigations of the savonius turbine with deformable-blades. *Energies* **2020**, *13*, 3717. [CrossRef]
26. Obidowski, D.; Stajuda, M.; Sobczak, K. Efficient Multi-Objective CFD-Based Optimization Method for a Scroll Distributor. *Energies* **2021**, *14*, 377. [CrossRef]
27. Fodemski, T.; Górecki, G.; Jasiński, P. Corrugated channels heat transfer efficiency Analysis based on velocity fields resulting from computer simulation and PIV Measurements. In Proceedings of the 8th International Conference on Heat Transfer, Fluid Mechanics and Thermodynamics, HEFAT, Pointe Aux Piments, Mauritius, 11–13 July 2011.
28. Li, X.-W.; Meng, J.-A.; Guo, Z.-Y. Turbulent flow and heat transfer in discrete double inclined ribs tube. *Int. J. Heat Mass Transf.* **2009**, *52*, 962–970. [CrossRef]
29. Di Piazza, I.; Ciofalo, M. Numerical prediction of turbulent flow and heat transfer in helically coiled pipes. *Int. J. Therm. Sci.* **2010**, *49*, 653–663. [CrossRef]

30. Eiamsa-Ard, S.; Wongcharee, K.; Sripattanapipat, S. 3-D Numerical simulation of swirling flow and convective heat transfer in a circular tube induced by means of loose-fit twisted tapes. *Int. Commun. Heat Mass Transf.* **2009**, *36*, 947–955. [CrossRef]
31. Manual ANSYS-CFX, Release 2020 R2. Available online: http://www.ansys.com (accessed on 15 July 2020).
32. Celik, I.B.; Ghia, U.; Roache, P.J.; Freitas, C.J.; Coleman, H.; Raad, P.E. Procedure for estimation and reporting of uncertainty due to discretization in CFD applications. *J. Fluids Eng. Trans. ASME* **2008**, *130*, 78001–78004. [CrossRef]
33. Bejan, A. *Convection Heat Transfer*, 4th ed.; John Wiley & Sons, Inc.: Hoboken, NJ, USA, 2013. [CrossRef]
34. Holman, J.P. *Heat Transfer*, 10th ed.; McGraw-Hill, Inc.: New York, NY, USA, 2010.
35. Swamee, P.K.; Jain, A.K. Explicit Equations for Pipe-Flow Problems. *J. Hydraul. Div.* **1976**, *102*, 657–664. [CrossRef]
36. Moody, L.F. Friction Factors for Pipe Flow. *Trans. Am. Soc. Mech. Eng.* **1944**, *66*, 671–681.
37. Wang, C.C.; Chiou, C.B.; Lu, D.C. Single-phase heat transfer and flow friction correlations for microfin tubes. *Int. J. Heat Fluid Flow* **1996**, *17*, 500–506. [CrossRef]